0026-895X/06/6902-576–587$20.00
MOLECULAR PHARMACOLOGY
Copyright © 2006 The American Society for Pharmacology and Experimental Therapeutics
Mol Pharmacol 69:576–587, 2006

Vol. 69, No. 2
18812/3080742
Printed in U.S.A.

Functional Properties of Internalization-Deficient $P2X_4$ Receptors Reveal a Novel Mechanism of Ligand-Gated Channel Facilitation by Ivermectin

Estelle Toulmé, Florentina Soto,[1] Maurice Garret, and Eric Boué-Grabot

Centre National de la Recherche Scientifique-Unité Mixte de Recherche 5543, Université Victor Segalen Bordeaux 2, Bordeaux, France (E.T., M.G., E.B.-G.); and the Max-Planck Institute for Experimental Medicine, Göttingen, Germany (F.S.)

Received September 12, 2005; accepted November 10, 2005

ABSTRACT

Although P2X receptors within the central nervous system mediate excitatory ATP synaptic transmission, the identity of central ATP-gated channels has not yet been elucidated. $P2X_4$, the most widely expressed subunit in the brain, was previously shown to undergo clathrin-dependent constitutive internalization by direct interaction between activator protein (AP)2 adaptors and a tyrosine-based sorting signal specifically present in the cytosolic C-terminal tail of mammalian $P2X_4$ sequences. In this study, we first used internalization-deficient $P2X_4$ receptor mutants to show that suppression of the endocytosis motif significantly increased the apparent sensitivity to ATP and the ionic permeability of $P2X_4$ channels. These unique properties, observed at low channel density, suggest that interactions with AP2 complexes may modulate the function of $P2X_4$ receptors. In addition, ivermectin, an allosteric modulator of several receptor channels, including mammalian $P2X_4$, did not potentiate the maximal current of internalization-deficient rat or human $P2X_4$ receptors. We demonstrated that binding of ivermectin onto wild-type $P2X_4$ channels increased the fraction of plasma membrane $P2X_4$ receptors, whereas surface expression of internalization-deficient $P2X_4$ receptors remained unchanged. Disruption of the clathrin-mediated endocytosis with the dominant-negative mutants Eps15 or AP-50 abolished the ivermectin potentiation of wild-type $P2X_4$ channel currents. Likewise, ivermectin increased the membrane fraction of nicotinic α7 acetylcholine (nα7ACh) receptors and the potentiation of acetylcholine current by ivermectin was suppressed when the same dominant-negative mutants were expressed. These data showed that potentiation by ivermectin of both $P2X_4$ and nα7ACh receptors was primarily caused by an increase in the number of cell surface receptors resulting from a mechanism dependent on clathrin/AP2-mediated endocytosis.

ATP mediates fast excitatory neurotransmission in the peripheral and central nervous system through direct activation of P2X receptors. ATP P2X receptors form a family of nonselective cation channels (North, 2002) composed of at least seven subunits ($P2X_{1-7}$). Among these subunits, the $P2X_4$ subtype is the most widely distributed in the brain, displaying some regional and cellular overlapping distribution with $P2X_2$ or $P2X_6$ subunits (Norenberg and Illes, 2000). The localization of $P2X_4$ subunits at postsynaptic specialization of hippocampal or cerebellar neurons (Rubio and Soto, 2001) as well as at axon terminals (Le et al., 1998) suggests a pivotal role for $P2X_4$-containing receptors in fast ATP synaptic transmission or the modulation of neurotransmitter release. However, the functional properties of postsynaptic ATP-mediated responses found in the brain do not correlate with those of any recombinant P2X receptors formed by combination of these subunits. For instance, recombinant mammalian $P2X_4$ receptors are moderately desensitizing $\alpha\beta$-methylene-ATP-insensitive channels (for review, North, 2002). Moreover, mammalian $P2X_4$ receptors are the only known ATP-gated ion channels to be modulated by ivermectin (Khakh et al., 1999b), an agonist of glutamate-gated chloride channels of invertebrates widely used in medicine against filarial diseases (Cully et al., 1994). In contrast, in hippocampus CA1 or brainstem neurons in which $P2X_4$ subunits are abundant, native ATP responses are elicited by $\alpha\beta$-methylene-ATP and are ivermectin-insensitive (Khakh et al., 1999b; Pankratov et al., 2002). These discrepancies, at-

This work was supported by Centre National de la Recherche Scientifique, Université Victor Segalen Bordeaux 2, Région Aquitaine, and by the Deutsche Forschungsgemeinschaft (So 390-1/2). E.T. is a recipient of a postgraduate fellowship from the Ministère de l'Education Nationale et de la Recherche.

[1] Current affiliation: Department of Pharmacological and Physiological Science, St. Louis University Medical School, St. Louis, MO.

Article, publication date, and citation information can be found at http://molpharm.aspetjournals.org.
doi:10.1124/mol.105.018812.

ABBREVIATIONS: AMPA, α-amino-3-hydroxy-5-methyl-4-isoazolepropionic acid; AP, activator protein; nα7AChr, nicotinic α7 acetylcholine; HEK, human embryonic kidney; ACh, acetylcholine; GFP, green fluorescent protein; NMDG, *N*-methyl-D-glucamine; DMSO, dimethyl sulfoxide; WT, wild type; DN, dominant negative; α7-GFP, expressed GFP-tagged α7.

tributed either to the expression of as yet unidentified subunits, heteromerization, or post-translation modification, showed that the identity of central P2X receptors remains to be deciphered (Khakh et al., 1999b; Norenberg and Illes, 2000).

There is currently accumulating evidence that ligand-gated channels from the "cys loop"- or glutamate-receptor family interact with many intracellular proteins implicated in the regulation of the number, subcellular localization, and anchoring of receptors (Moss and Smart, 2001; Mayer, 2005). In addition, receptor-associated proteins have been shown to modulate functional properties of ligand-gated channels. Microtubule-associated protein MAP1B (Billups et al., 2000) or GABA receptor-associated protein (Chen et al., 2000) modulate the agonist sensitivity and/or kinetics of GABA-gated channels, whereas postsynaptic density 95 accelerates the rate of recovery from desensitization of GluR6 (Bowie et al., 2003). In comparison, very little is known about neuronal P2X receptor-associated proteins. Recent studies on trafficking of P2X receptors demonstrated convincingly that $P2X_4$ receptors cycle into and out of the plasma membrane, providing a means of modulating receptor density (Bobanovic et al., 2002). Other ligand-gated channels such as $GABA_A$ or AMPA receptors undergo regulated cycling. This has been shown to modulate excitatory and inhibitory transmission (Kittler et al., 2000; Carroll et al., 2001). Rat $P2X_4$ receptors interact directly with μ2 (also called AP-50) subunits of AP2 adaptor complex through a novel tyrosine-based sorting signal at the C-terminal tail of $P2X_4$ subunits (Royle et al., 2002, 2005), which ensures the recruitment and selection of $P2X_4$ receptors for their constitutive- and agonist-dependent internalization (Bobanovic et al., 2002; Royle et al., 2002). This YxxGL motif is totally conserved among mammalian $P2X_4$ sequences but is absent from other P2X subtypes. Mutation of the binding site for AP2 on $P2X_4$ causes a decrease in internalization and a resulting dramatic increase in the surface expression of $P2X_4$ receptors (Royle et al., 2005). In this study, we examined whether interaction with AP2 influenced the functional properties of $P2X_4$ channels using internalization-deficient rat or human $P2X_4$ channels. Disruption of AP2/$P2X_4$ interaction produced unique $P2X_4$ receptor functional properties consistent with those of native P2X responses. Furthermore, in the absence of interaction with AP2, $P2X_4$ channels were found to be insensitive to ivermectin. In this study, we demonstrated that the binding of ivermectin onto receptors increased the number of surface $P2X_4$ channels (as well as nicotinic α7 acetylcholine receptors) and that this regulatory effect of ivermectin could be disrupted by interfering with clathrin/AP2-mediated endocytosis process.

Materials and Methods

Molecular Biology. Wild-type rat $P2X_4$ and rat α7 nicotinic acetylcholine (kindly provided by Dr. P. Séguéla, Montreal Neurological Institute, Montreal, QC, Canada) plasmids were used in this work, but some experiments were reproduced with wild-type or mutated human $P2X_4$ receptors (specified in the text). Receptor mutants were generated by polymerase chain reaction with the wild-type plasmid as a DNA template using PfuTurbo DNA polymerase (Stratagene, La Jolla, CA) to minimize artifactual mutations. Point mutations were constructed using the Quickchange site-directed mutagenesis system (Stratagene). For construction of C-terminal-truncated rat $P2X_4$ receptors ($P2X_4$ Δ377), we used a 3′ primer derived from the amino acid sequence R^{368}DK KYKYVED^{377} of $P2X_4$ followed by an artificial stop codon and a terminal XbaI site. Tagged-$P2X_4$ and -α7 subunits were generated as reported previously for other subunits (Boué-Grabot et al., 2004a). Plasmids encoding the dominant-negative Eps15 mutant (Eps 15 DN or GFP-ED95/295) and a control construct (Eps15 control, also called GFP-DIIID2; Benmerah et al., 1996) were provided by Dr. Agnès Hémar (Centre National de la Recherche Scientifique-Unité Mixte de Recherche 5091, Bordeaux, France). The cDNA coding for rat μ2 (or AP-50) was generated with RNA extracted from the brain by reverse transcription-polymerase chain reaction. The dominant-negative AP-50 subunit was made by sequentially mutating D^{176}A and W^{421}A as described previously (Nesterov et al., 1999; Royle et al., 2002). All constructs were subcloned into $pcDNA_3$ (Invitrogen, Carlsbad, CA) and verified by automatic dideoxy DNA sequencing (MWG Biotech, High Point, NC).

***Xenopus laevis* Oocyte Injection and Electrophysiology.** Oocytes were prepared as described previously (Boué-Grabot et al., 2004a). Stage V and VI oocytes were manually defolliculated before nuclear injection (Nanoject II; Drummond Scientific, Broomall, PA) of cDNAs. The oocytes were then incubated in Barth's solution containing 1.8 mM $CaCl_2$ and gentamycin (10 μg/ml; Sigma-Aldrich, St. Louis, MO) at 19°C for 1 to 4 days before electrophysiological recordings. Two-electrode voltage-clamp recordings were carried out at room temperature using glass pipettes (1–2 MΩ) filled with 3 M KCl solution to ensure a reliable holding potential. Oocytes were voltage clamped at −60 mV, and the membrane currents were recorded through an OC-725B amplifier (Warner Instruments, Hamden, CT) and digitized at 500 Hz. Oocytes were perfused at a flow rate of 10 to 12 ml/min with Ringer's solution (Na^+-R), pH 7.4, containing 115 mM NaCl, 5 mM NaOH, 2.5 mM KCl, 1.8 mM (or 0.1 mM) $CaCl_2$, and 10 mM HEPES or using an extracellular solution ($NMDG^+$-R) containing 5 mM NaCl, 110 mM NMDG, 5 mM NaOH, 2.5 mM KCl, 0.1 mM $CaCl_2$, and 10 mM HEPES (Boué-Grabot et al., 2004b). Agonists and drugs (purchased from Sigma-Aldrich) were prepared at their final concentration in the perfusion solution and applied using a computer-driven valve system (Ala Scientific, Westbury, NY). For all experiments, ivermectin was initially dissolved (10 mM) in DMSO and kept at −20°C for up to 2 weeks. The concentration of DMSO in the final solution was 0.03% ($P2X_4$ experiments) and 0.3% (α7 experiments). Application of the vehicle alone did not affect ATP or ACh responses.

Data Analysis. All data were analyzed using Prism 4.0 (GraphPad Software Inc., San Diego, CA). Numerical values are expressed as mean ± S.E.M. from n determination. Current-voltage relations were obtained by applying 200-ms voltage ramps from −80 to +50 mV. Reversal potentials (E_{REV}) were estimated from the I–V relationship, determined by linear regression test analysis. The ratio of $NMDG^+$ to Na^+ permeability (P) was calculated using the function $P_{NMDG^+}/P_{Na^+} = \exp(\delta E_{REV} F/RT)$ as described previously (Khakh et al., 1999a). δE_{REV} is the observed shift in reversal potential, F is the Faraday constant, R is the gas constant, and T is absolute temperature. Dose-response curves were fitted to the Hill sigmoidal equation, and EC_{50} values were determined by nonlinear regression analysis. Statistical comparisons were assessed using Student's t test. The differences were considered significant if $p < 0.05$.

Surface Biotinylation and Immunoblotting. Biotinylation experiments were performed essentially as described previously (Ennion and Evans, 2002). To examine the effect of ivermectin on surface receptor expression, 25 to 30 oocytes were incubated in Ringer's solution containing 0.5 mg/ml sulfo-*N*-hydroxysuccinimide-biotin (Pierce, Rockford, IL) and either ivermectin or DMSO (control) for 2 min at room temperature. Then, oocytes were immediately placed in a chilled Ringer-biotin solution for 30 min at 4°C with gentle agitation. After washing four times in Ringer's solution, oocytes were homogenized in a volume of 20 μl/oocyte of buffer H (10 mM HEPES, 0.3 M sucrose, protease inhibitor cocktail; Roche Diagnostics, Indianapolis, IN), and solubilized with 1% Triton X-100 at 4°C for 2 h.

After centrifugation (4°C) at 10,000*g* for 10 min, 7.5 to 15 μl of the supernatant was stored at −20°C before SDS-PAGE to assess total receptor fraction. The remaining supernatant was incubated at 4°C for 4 h with 40 μl of Immunopure Immobilized Neutravidin binding proteins (Pierce) to precipitate surface proteins. Beads were washed four times with buffer H, and adsorbed proteins were eluted with 1 volume of SDS sample buffer at room temperature. Surface and total proteins were separated on SDS-PAGE and revealed by Western blotting using either anti-$P2X_4$ receptor antibodies at a 1:4000 dilution (0.25 μg/ml; Nicke et al., 2005) or anti-GFP antibodies at a 1:8000 dilution (Invitrogen). Quantification of Western blots was performed using Image J 1.33u (http://rsb.info.nih.gov/nih-image/Default.html) software, and surface-total protein ratio was related to the number of oocytes (on average, total protein bands corresponded to 0.37 to 0.75 oocytes, and surface signals corresponded to 20 oocytes).

Results

Mutation of the Endocytosis Motif of $P2X_4$ Receptors Increases Functional Receptors in Oocytes. Royle et al. (2002, 2005) identified a C-terminal $P2X_4$ motif (Y^{378}xxGL^{382}) of interaction with AP-50 (also called μ2) protein of the AP2 complex required for the constitutive endocytosis of $P2X_4$ receptors. This motif is conserved among the mammalian $P2X_4$ sequences but is absent in other P2X subtypes. Mutation of this sorting signal increased the surface expression of $P2X_4$ receptors 5- to 8- fold in transfected neurons (Royle et al., 2002). We eliminated the site of interaction with AP2 of rat $P2X_4$ subunit sequence either by truncating at residue 377 ($P2X_4$ Δ377) or replacing tyrosine 378 by an alanine ($P2X_4$ Y378A). Two days after the injection of 1.5 ng of cDNAs encoding wild-type $P2X_4$, $P2X_4$ Δ377, or $P2X_4$ Y378A in *X. laevis* oocytes, ATP-evoked inward currents recorded by two-electrode voltage clamp displayed moderately desensitizing kinetics for all channels tested (Fig. 1A). However, the desensitization rate of truncated $P2X_4$ receptors was more variable than for wild-type or $P2X_4$ Y378A receptors; 24 to 63% of the oocytes (four different batches) expressing truncated $P2X_4$ receptors displayed a slowly desensitizing phenotype (see Fig. 1A, inset). Variation of phenotype was previously reported with C-terminal-truncated $P2X_2$ receptor (Boué-Grabot et al., 2000). The amplitude of ATP current was, respectively, 0.27 ± 0.06 μA (n = 20), 7.44 ± 0.45 μA (n = 21), and 7.41 ± 0.66 μA (n = 9) for $P2X_4$ WT, $P2X_4$ Δ377, and $P2X_4$ Y378A (Fig. 1A), revealing a large (25-fold) increase in the functional response of mutated $P2X_4$ subunits. A 10-fold increase in current amplitude was similarly observed when oocytes injected with 1.5 ng of cDNAs coding for human $P2X_4$ Y378A (I_{ATP} = 12.94 ± 2.1 μA, n = 8) or human $P2X_4$ WT (I_{ATP} = 1.28 ± 0.48 μA, n = 9) were compared. The enhancement of maximal current was dependent on the amount of DNA injected (Fig. 1B) but was independent of the time course of channel expression (Fig. 1C). Data in Fig. 1B indicated that 30 times less DNA was necessary to reach maximal current of $P2X_4$ Δ377 versus $P2X_4$ WT. According to previous data that demonstrated that disruption of interaction with AP2, inferred by mutated $P2X_4$ receptors, increased the number of surface $P2X_4$ receptors in transfected HEK cells or neurons (Bobanovic et al., 2002; Royle et al., 2002), the observed increases in maximal current are probably related to a higher surface expression of mutated $P2X_4$ receptors.

Functional Characterization of Endocytosis-Deficient $P2X_4$ Receptors. ATP-induced currents in oocytes expressing wild-type or mutant $P2X_4$ channels fully recovered after repeated applications at 4-min intervals (not shown). High density of $P2X_2$ channels was shown to alter

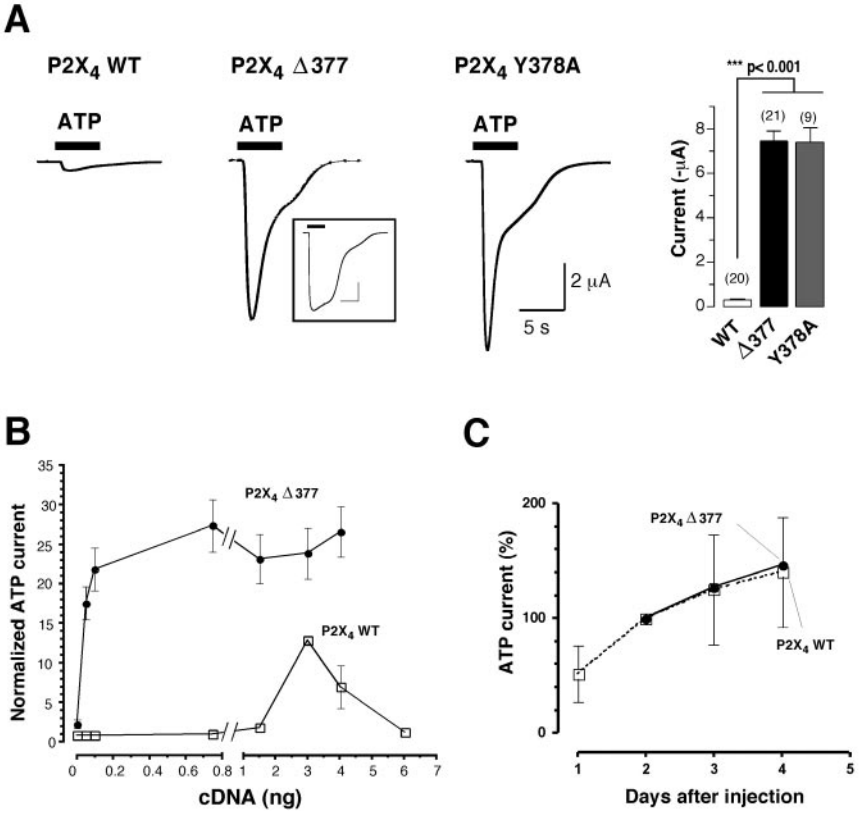

Fig. 1. Mutation of the endocytosis motif of $P2X_4$ receptors increases ATP current density. A, representative currents from oocytes expressing rat $P2X_4$ WT, $P2X_4$ Δ377, or $P2X_4$ Y378A receptors in response to 5-s application of 100 μM ATP. Deletion ($P2X_4$ Δ377) or mutation ($P2X_4$Y378A) of $P2X_4$ receptor endocytosis motif significantly increased the amplitude of current in comparison with $P2X_4$ WT receptors (***, $p < 0.001$). Recordings were performed the same day (2 days after injection of 1.5 ng of each cDNA). Note in the inset the slow desensitizing kinetics observed in 24 to 63% oocytes expressing $P2X_4$ Δ377. B, amplitude of 100 μM ATP currents recorded 2 days after nuclear injection in *X. laevis* oocytes of different quantities of cDNAs encoding $P2X_4$ WT (□) or $P2X_4$ Δ377 (●). Mean peak currents were normalized to the response of oocytes injected with 1.5 ng of $P2X_4$ WT cDNA; n = 4 and 20. C, time course of $P2X_4$ WT (□) or $P2X_4$ Δ377 currents (●) respectively normalized to the mean of currents recorded at day 2 (n = 7–13). Holding potential was −60 mV.

channel properties in oocytes (Fujiwara and Kubo, 2004). To analyze functional properties of internalization-deficient P2X$_4$ receptors and rule out the possibility of density-dependent changes, wild-type and mutant rat P2X$_4$ receptors were expressed at similar low levels by injecting, respectively, 1.5 and 0.1 ng of cDNA encoding subunits. Unless specified, the following experiments were performed under these conditions. The current-voltage relationship was determined by measuring the peak of ATP (100 μM) response obtained at several membrane potentials (from −60 to 20 mV, n ranged from 2 to 5) and normalized to the current obtained at −60 mV. Superimposed I–V curves for WT and mutated P2X$_4$ channels with reversion potential of −8.1 ± 6.6 and −9.0 ± 7.2 mV, respectively, showed that mutation did not change the cation selective permeability of P2X$_4$ channels (Fig. 2A). Concentration-response curves for oocytes expressing either P2X$_4$ or P2X$_4$ Y378A at a similar current density (I_{ATP} < 6 μA at saturating concentration) were obtained by recording activity of both channels at different concentrations of ATP. EC_{50} of ATP was found to be 0.29 ± 0.15 μM and 4.32 ± 1.4 μM, respectively, for P2X$_4$ Y378A and wild-type P2X$_4$ channels (Fig. 2B; n ranged from 4 to 12), indicating that P2X$_4$ Y378A receptors were 15 times more sensitive to ATP than wild-type receptors. Rat P2X$_4$ channels are typically considered insensitive to $\alpha\beta$-methylene-ATP, although a slight effect at concentrations higher than 100 μM has been reported (Khakh et al., 1999b; Jones et al., 2000; North, 2002). As illustrated in Fig. 2C, $\alpha\beta$-methylene-ATP evoked measurable currents only at concentrations superior to 100 μM for wild-type P2X$_4$, representing 15% of 100 μM ATP currents. Similar results were observed for P2X$_4$ Y378A channels (I_{ATP} = 6.7 ± 0.7 μA, n = 12; Fig. 2C). It is noteworthy that at a

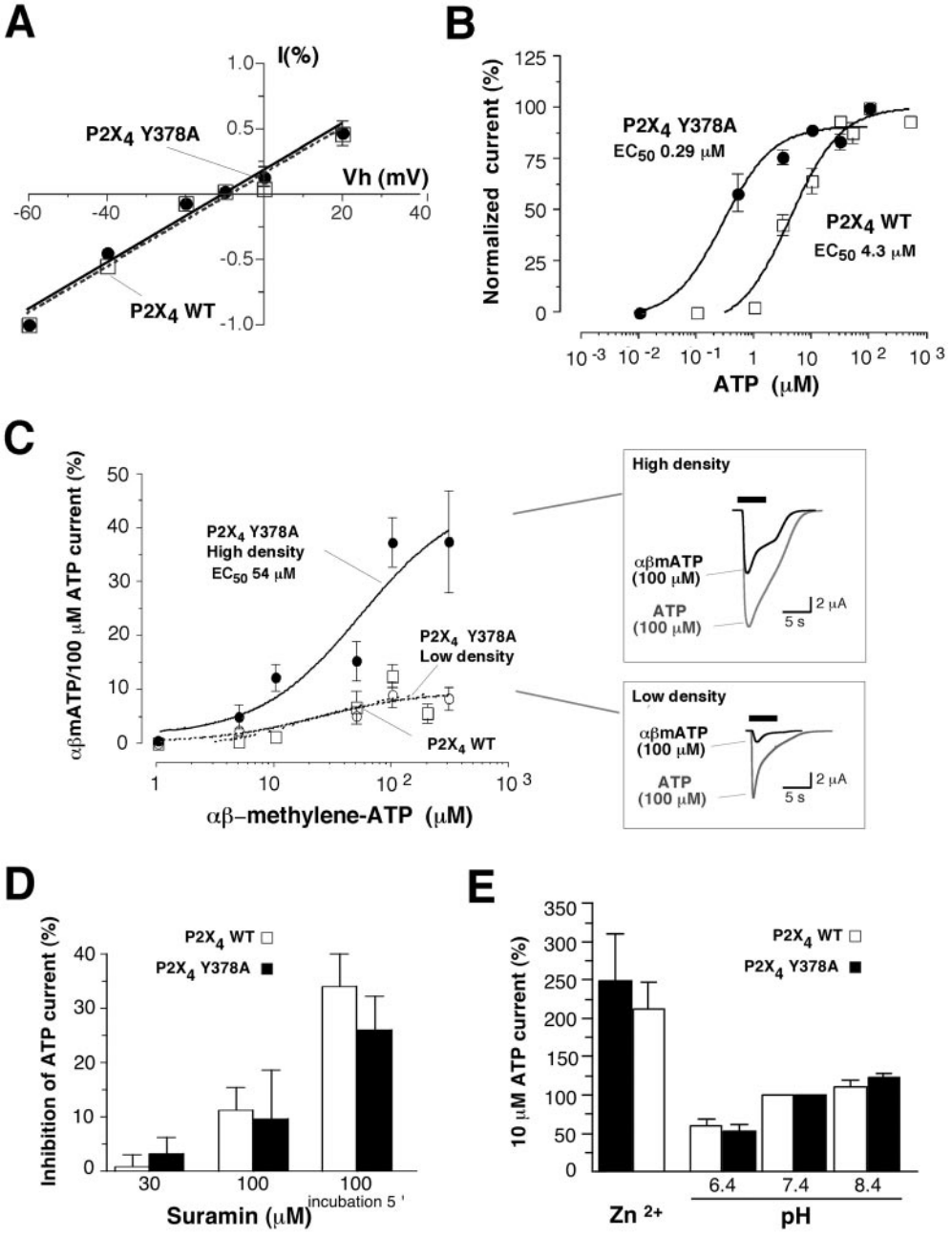

Fig. 2. Functional properties of endocytosis-deficient P2X$_4$ channels expressed in *X. laevis* oocytes. A, current-voltage relationships of wild-type P2X$_4$ (□) or P2X$_4$ Y378A (●) receptors. Currents evoked by 100 μM ATP were normalized to the current recorded at a holding potential of −60 mV. B, ATP dose-response curves of P2X$_4$ WT (□, n = 4–12) and P2X$_4$ Y378A (●, n = 4–12) receptors normalized to 100 μM ATP-induced current. Current density was similar for both channels. C, concentration-effect curves for $\alpha\beta$-methylene-ATP at low density (I_{ATP} < 7 μA, □ and ○, respectively, for WT- and mutated-P2X$_4$) or at high density (●, I_{ATP} > 10 μA for P2X$_4$ Y378A receptors). $\alpha\beta$-Methylene-ATP-induced currents were normalized to 100 μM ATP responses. Insets, superimposition of representative currents evoked either by ATP or $\alpha\beta$-methylene-ATP (100 μM each) for oocytes expressing P2X$_4$ WT at low density or P2X$_4$ Y378A receptors at high density. D, inhibition of 10 μM ATP currents induced by coapplication of suramin (30 or 100 μM) or 5-min preincubation of 100 μM suramin (n = 2–5). E, mean peak currents evoked by 10 μM ATP at pH 6.4, 7.4, or 8.4 or by 10 μM ATP at pH 7.4 in the presence of 10 μM Zn^{2+}. Currents are normalized to the value obtained at pH 7.4 in the same cell (n = 5–7).

higher density of $P2X_4$ Y378A channels (I_{ATP} = 13 ± 0.8 μA, n = 11), αβ-methylene-ATP evoked robust responses, representing 40% of ATP currents. The dose-response curve displayed an EC_{50} of 54 ± 3 μM, demonstrating that αβ-methylene-ATP was a potent agonist of $P2X_4$ Y378A channels depending on the channel density (Fig. 2C).

Suramin is an antagonist of P2X receptors with low efficacy on $P2X_4$ receptors (North, 2002; Fig. 2D). Coapplication or preincubation (5 min) of the antagonist (tested at 30 and 100 μM) reduced ATP-induced response by a maximum of 33.8 ± 0.6% or 25.9 ± 6.6% (n = 2–5, $p > 0.05$) respectively for wild-type and mutant $P2X_4$ channels, indicating that mutation produced no change in suramin efficacy. Moreover, as summarized in Fig. 2E, mutation of the endocytic motif did not modify neither the well established potentiation by Zn^{2+} (10 μM; Soto et al., 1996) nor the pH dependence of the action of ATP on $P2X_4$ channels (North, 2002).

Dilation Properties of Endocytosis-Deficient $P2X_4$ Receptors. $P2X_4$ channels undergo permeability changes during prolonged or repetitive activation (Khakh et al., 1999a; Virginio et al., 1999). As reported and illustrated in Fig. 3, A and B, application of ATP (100 μM) in low-Ca^{2+} Ringer's solution opens in milliseconds a channel permeable to small cations (state I_1) and, then, in the continuous presence of ATP, the channel becomes permeable to much larger cations (state I_2). I_2 represented 241.8 ± 77.22% (n = 6) of I_1 for wild-type $P2X_4$ receptors (Fig. 3D). We tested whether $P2X_4$ Y378A channels underwent permeability changes. We found that prolonged application (2 min) of ATP evoked biphasic $P2X_4$ Y378A currents. Contrary to $P2X_4$WT, I_2 represented only 35.1 ± 10.2% (n = 7) of I_1 for $P2X_4$ Y378A channels (Fig. 3, A, B, and D). We determined the reversal potential of ATP-evoked current as a function of the time either in Na^+-R solution or with $NMDG^+$ replacing all the extracellular Na^+ (Fig. 3C). The reversal potentials for both channels in Na^+-R solution of I_1 were constant and close to 0 mV (Fig. 3E). The reversal potential of $P2X_4$ WT in $NMDG^+$ solution shifted by ~22 mV from −59.9 ± 7.3 mV (state I_1) to −37.5 ± 1.9 mV (state I_2) during ATP application in $NMDG^+$-R solution, showing the progressive permeability increase of $P2X_4$ WT channel pore (Fig. 3E). The reversal potential of I_1 current for $P2X_4$ Y378A was −21.2 ± 0.7 mV and then slightly decreased to −24 ± 2 mV at the entry in I_2 state (0.5 min in ATP; Fig. 3C). These results showed that $P2X_4$ Y378A receptors are immediately permeable to $NMDG^+$, suggesting that cytosolic domains played an important role in permeability change (Fisher et al., 2004). Although no significant increase in $NMDG^+$ permeability occurred during prolonged ATP application (Fig. 3E), $P2X_4$ Y378A displayed biphasic responses showing that transition between I_1 and I_2 states is a complex mechanism that not only reflects changes in permeability.

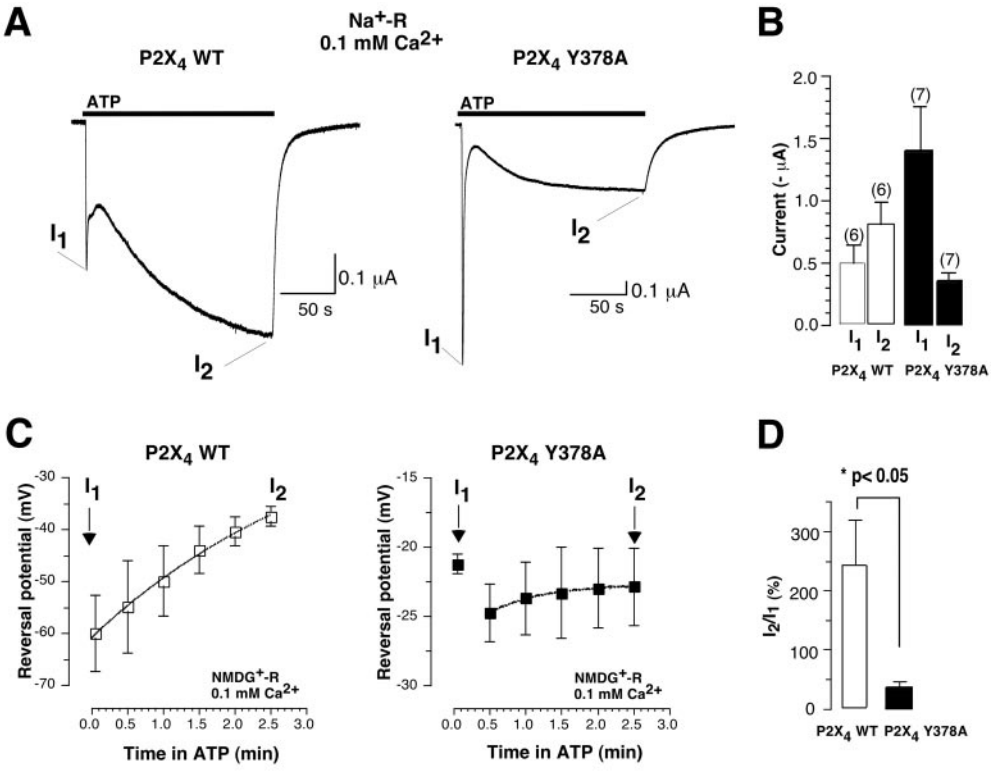

Fig. 3. Permeability changes of endocytosis-deficient $P2X_4$ receptors. A, representative biphasic currents (I_1 and I_2) elicited by prolonged application of 100 μM ATP in Ringer's solution containing 0.1 mM Ca^{2+} from oocytes expressing $P2X_4$ WT or $P2X_4$ Y378A receptors at low-current density. The first peak (I_1) develops rapidly and desensitizes; the second peak (I_2) develops slowly over several minutes. B, mean amplitudes of I_1 and I_2 currents (microamperes) from experiments described in A. D, I_2/I_1 ratio is significantly decreased for $P2X_4$ Y378A receptors (n = 7) compared with $P2X_4$ WT receptors (n = 6); *, $p < 0.05$. C, time course of reversal potential change in $NMDG^+$ Ringer's solution. Each point represented the mean ± S.E.M. (n = 4–6) of the reversal potential obtained from voltage ramps (−80 to + 50 mV; 200 ms). E, table summarizing reversal potentials, shifts in reversal potentials, and the relative permeability P_{NMDG+}/P_{Na+} of $P2X_4$ WT or $P2X_4$ Y378A I_1 and I_2 conducting states in $NMDG^+$ or Na^+ Ringer's solution.

E

	I_1			I_2			
	Erev (mV)		P_{NMDG^+}/P_{Na^+}	Erev (mV)		P_{NMDG^+}/P_{Na^+}	Change $NMDG^+$ Erev (mV)
	Na^+-R	$NMDG^+$-R		Na^+-R	$NMDG^+$-R		
$P2X_4$ WT	0	-59.9 ± 7.3	0.09 ± 0.03	0	-37.5 ± 1.9	0.23 ± 0.02	+ 22.5 ± 5.4
$P2X_4$ Y378A	0	-21.2 ± 0.7	0.43 ± 0.01	0	-22.8 ± 2.7	0.40 ± 0.04	no

Altogether, these results show that endocytosis motif is critical for P2X$_4$ function. These differences, observed at similar current densities, eliminated the possibility of density-dependent changes and suggested that loss of interaction with AP2 proteins modulates function of P2X$_4$ receptors.

Ivermectin Does Not Potentiate Endocytosis-Deficient P2X$_4$ Receptors. Ivermectin slows deactivation and increases maximum ATP currents through rat and human P2X$_4$ receptors but not through other P2X receptor subtypes (Khakh et al., 1999b; Priel and Silberberg, 2004). Figure 4, A and B, shows that 2-min application of ivermectin (3 μM) significantly increased ATP currents from oocytes expressing rat or human P2X$_4$ channels. However, we noticed that ivermectin potentiated ATP currents with an initial amplitude of less than 2 μA but had no significant effect on oocytes showing higher channel density ($I_{ATP} > 2$ μA; Fig. 4B, $n = 37$). This finding has not been reported in previous studies using both P2X$_4$ orthologs (Khakh et al., 1999b; Priel and Silberberg, 2004). In agreement with previous work (Khakh et al., 1999b), ivermectin increased the amplitude of initial ATP current ($I < 2$ μA; Fig. 4E) by 297 ± 21% or 287 ± 64% for rat or human P2X$_4$ WT channels, respectively. In contrast, ivermectin (3 or 10 μM) failed to increase the peak current of rat or human P2X$_4$ Y378A and rat P2X$_4$ Δ377 at all current densities tested (I_{ATP} ranged from 0.1 to 10 μA, $n = 53$; Fig. 4, C and D). After preincubation with 3 μM ivermectin, ATP current represented 141 ± 18% ($n = 11$), 76 ± 11% ($n = 6$), or 133 ± 17% ($n = 10$) of the initial ATP responses, respectively, for rat, human P2X$_4$ Y378A, or rat P2X$_4$ Δ377 (to compare wild-type and mutant P2X$_4$, only $I_{ATP} < 2$ μA were taken into account). However, it is important to note that the deactivation rate of wild-type and both mutated channels was slowed by ivermectin (Fig. 4, A and C). These observations, in agreement with previous studies (Khakh et al., 1999b; Priel and Silberberg, 2004), showed that the maximal current increase and the deactivation slowdown induced by ivermectin result from distinct mechanisms on mammalian P2X$_4$ channels. The surprising result show-

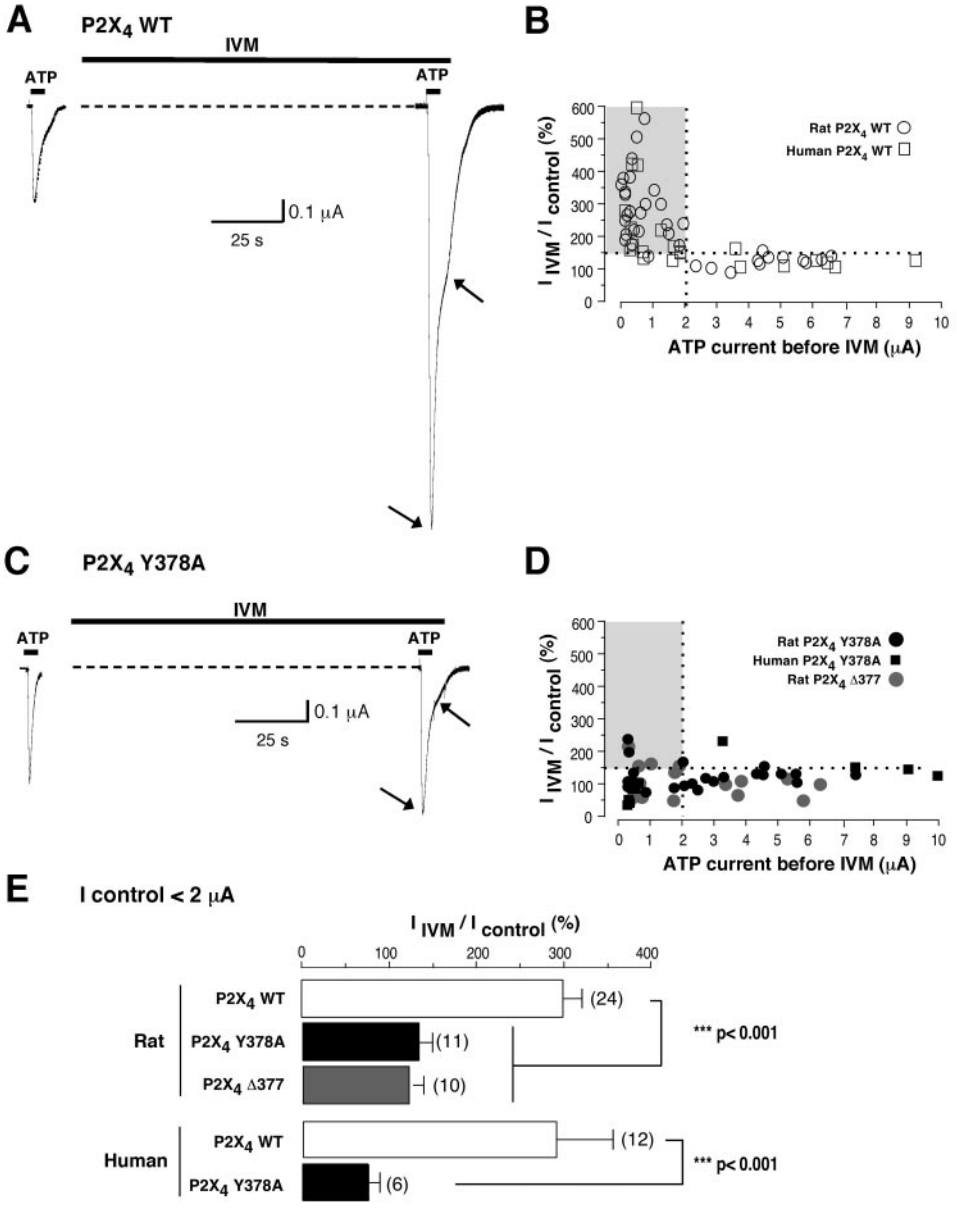

Fig. 4. Ivermectin does not potentiate mutated rat or human P2X$_4$ receptor peak current. A and C, representative currents elicited by ATP (100 μM) before and after 2-min preincubation with 3 μM ivermectin (IVM). A, 2-min preapplication of IVM (3 μM) produced a large increase in rat P2X$_4$ WT channel currents induced by 100 μM ATP and slowed deactivation (arrows). B, potentiation by IVM (3 μM) of rat or human P2X$_4$ WT peak current (gray panel) occurred when initial ATP current was inferior to 2 μA ($n = 24$). No potentiation was observed for higher initial ATP current ($I > \mu$A, $n = 13$). C, IVM produced no significant increase in ATP peak current of rat P2X$_4$ Y378A receptors but slowed the rate of deactivation of P2X$_4$ Y378A channels (arrows). D, IVM induced no significant effect on ATP currents whatever the amplitude of initial ATP responses for rat or human P2X$_4$ Y378A and rat P2X$_4$ Δ377 receptors. E, means of potentiation by IVM. Only oocytes with initial ATP responses < to 2 μA were taken in account.

ing that endocytosis motif was required for the peak current potentiation by ivermectin (Fig. 4) and the intriguing fact that functional properties of internalization-deficient $P2X_4$ receptor mutants (Figs. 2 and 3) were similar to those observed for wild-type $P2X_4$ receptors in the presence of ivermectin (Khakh et al., 1999) leads us to hypothesize that ivermectin caused potentiation by increasing the number of surface receptors.

The Functional Potentiation of $P2X_4$ Receptors by Ivermectin Is Accompanied by an Increase in Receptor Surface Expression. To directly test whether an increase in the number of surface receptors could underlie the ivermectin effect on $P2X_4$ channels, we examined the relative amount of surface-specific protein expression by conducting surface biotinylation experiments on oocytes expressing $P2X_4$ receptors. Detection of total and surface $P2X_4$ subunits using a C-terminal $P2X_4$-specific antibody (Nicke et al., 2005) revealed the weak surface expression of $P2X_4$ receptors (Fig. 5A). Surface fraction represented ~0.3% of total $P2X_4$ proteins under control conditions (Fig. 5A, lane C). In the presence of 3 μM ivermectin (2- or 30-min incubation), we observed a significant increase in surface signals, whereas total $P2X_4$ expression remained unchanged (Fig. 5, A and D). Comparison of the relative surface/total ratio in the absence or the presence of ivermectin indicated that ivermectin increased plasma membrane $P2X_4$ subunits by 300 to 450% (for 30- or 2-min incubation, respectively, four independent experiments). The increase induced by ivermectin was not attributable to the presence of DMSO because control oocytes were incubated in Ringer's solution containing 0.03% DMSO. The absence of signal from noninjected oocytes (Fig. 5A, lanes NI) or oocytes expressing either $P2X_4$ Δ377 or $P2X_4$ Y378A (Fig. 5B) demonstrated the specific detection of wild-type $P2X_4$ and suggested that the residue Y^{378} is critical for the C-terminal antigenicity. Contrary to $P2X_4$ WT, we showed, using anti-GFP antibodies, that similar ivermectin treatment had no effect on the relative surface fraction of $P2X_4$ Y378A-yellow fluorescent protein receptors (Fig. 5, C and D). These results provide evidence that the 3-fold potentiation of $P2X_4$ currents caused by ivermectin can be accounted for by an increase in the number of surface receptors.

Up-Regulation by Ivermectin Is Driven by Endocytosis. The rapid time course of the ivermectin-induced increase of $P2X_4$ receptors expression on the plasma membrane limits the mechanism through which it could occur (e.g., trafficking rather than receptor synthesis or assembly). To test whether the effect of ivermectin on wild-type $P2X_4$ channels involved AP2/clathrin-dependent endocytosis, we disrupted the clathrin-mediated pathway using well characterized dominant-negative mutants of endocytosis. We first coinjected oocytes with a mixture (1:1.5 ratio) of cDNAs encoding wild-type $P2X_4$ receptors and either the dominant-negative mutant of Eps15 (Eps15 DN) or a control Eps15 construct (Benmerah et al., 1996). The amplitude of ATP currents for $P2X_4$ receptors was significantly higher in the presence of Eps15 DN (I_{ATP} = 0.16 ± 0.03 μA, n = 7) compared with the Eps15 control (I_{ATP} = 0.07 ± 0.02 μA, n = 7), showing that Eps15 DN prevented the rapid endocytosis of $P2X_4$ receptors (Fig. 6, A, B, and E). Moreover, the potentiation of ATP current by ivermectin was significantly decreased in the presence of Eps15 DN (I_{ATP} after ivermectin represented 168.5 ± 26% of I_{ATP} control, n = 7), whereas $P2X_4$ potentiation is unaffected by the presence of Eps15

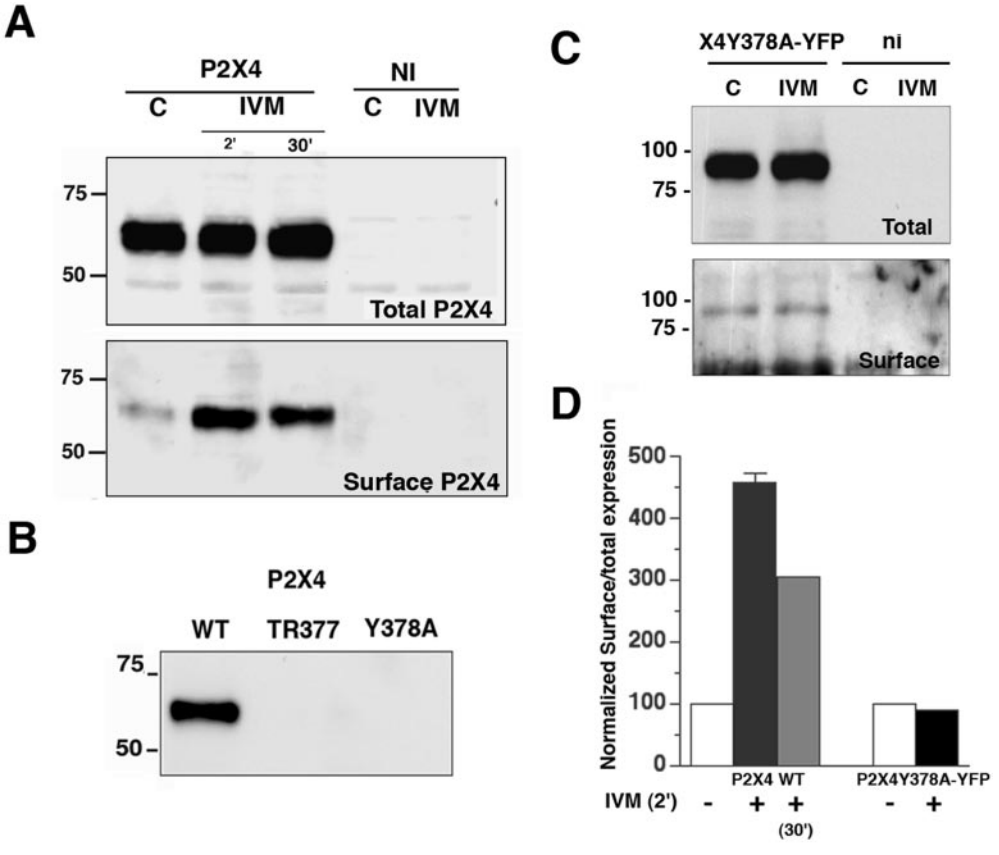

Fig. 5. Surface expression of $P2X_4$ WT receptors is increased by ivermectin. A, $P2X_4$ WT expressing or noninjected (NI) oocytes were incubated in ivermectin (3 μM) or in vehicle (c) 2- or 30-min before surface biotinylation. Representative Western blot shows $P2X_4$ immunoreactivity in total or surface biotinylated extracts from oocytes expressing $P2X_4$ WT, whereas no signal is detected from noninjected oocytes (NI). B, anti-$P2X_4$ antibodies directed against the C-terminal of $P2X_4$ receptors did not detect $P2X_4$ Δ377 or $P2X_4$ Y378A receptors in total protein extracts from oocytes in which functional expression was assessed by voltage-clamp recordings. C, anti-GFP Western blot on total extracts or biotinylated surface proteins from oocytes expressing $P2X_4$ Y378A-yellow fluorescent proteins. Oocytes were incubated in vehicle (c) or ivermectin (3 μM) 2 min before biotinylation. D, means of surface/total expression ratio from experiments described in A and C show that IVM (+) induced a dramatic increase in surface $P2X_4$ fraction, whereas surface expression of mutated $P2X_4$ receptors was unchanged.

control (I_{ATP} after ivermectin represented 347.1 ± 22.5%, n = 14 of I_{ATP} control; Fig. 6, A, B, and D).

We next used a dominant-negative mutant of the AP-50 subunit, a component of the AP2 complex (Nesterov et al., 1999; Royle et al., 2002), and showed that expression of P2X$_4$ receptors in oocytes was significantly higher in the presence of AP-50 DN compared with wild-type AP-50 (Fig. 6, C and D). Indeed, in cells coexpressing P2X$_4$ and wild-type AP-50 subunits, inward currents in response to ATP were rarely detectable, suggesting that P2X$_4$ receptors were predominantly retained in intracellular compartments (Fig. 6D). Similar to Eps15 DN, AP-50 DN abolished the ivermectin potentiation of ATP-induced P2X$_4$ peak currents (Fig. 6, C and E); after ivermectin, ATP-induced current represented 143.7 ± 25% of the control current (n = 10; Fig. 6E). As illustrated in Fig. 6, A to C, ivermectin slowed the deactivation rate of wild-type P2X$_4$ channels in the presence or absence of dominant-negative mutants, indicating that this effect of ivermectin is controlled by a different mechanism not involving constitutive internalization of P2X$_4$ receptors. Taken together, the results shown in Figs. 4 to 6 demonstrated that the peak current potentiation of P2X$_4$ channels by ivermectin is underlied by insertion of additional cell surface receptors which occurs by a mechanism involving constitutive AP2/clathrin-dependent internalization.

Ivermectin Increases the Number of Cell Surface nα7ACh Receptors by a Mechanism Involving Endocytosis. Preapplication of ivermectin enhances reversibly ACh-evoked current of nicotinic α7 acetylcholine receptors (nα7AChR) expressed in *X. laevis* oocytes and HEK cells (Krause et al., 1998). In addition, ivermectin increases the apparent affinity and cooperativity of the ACh dose-response

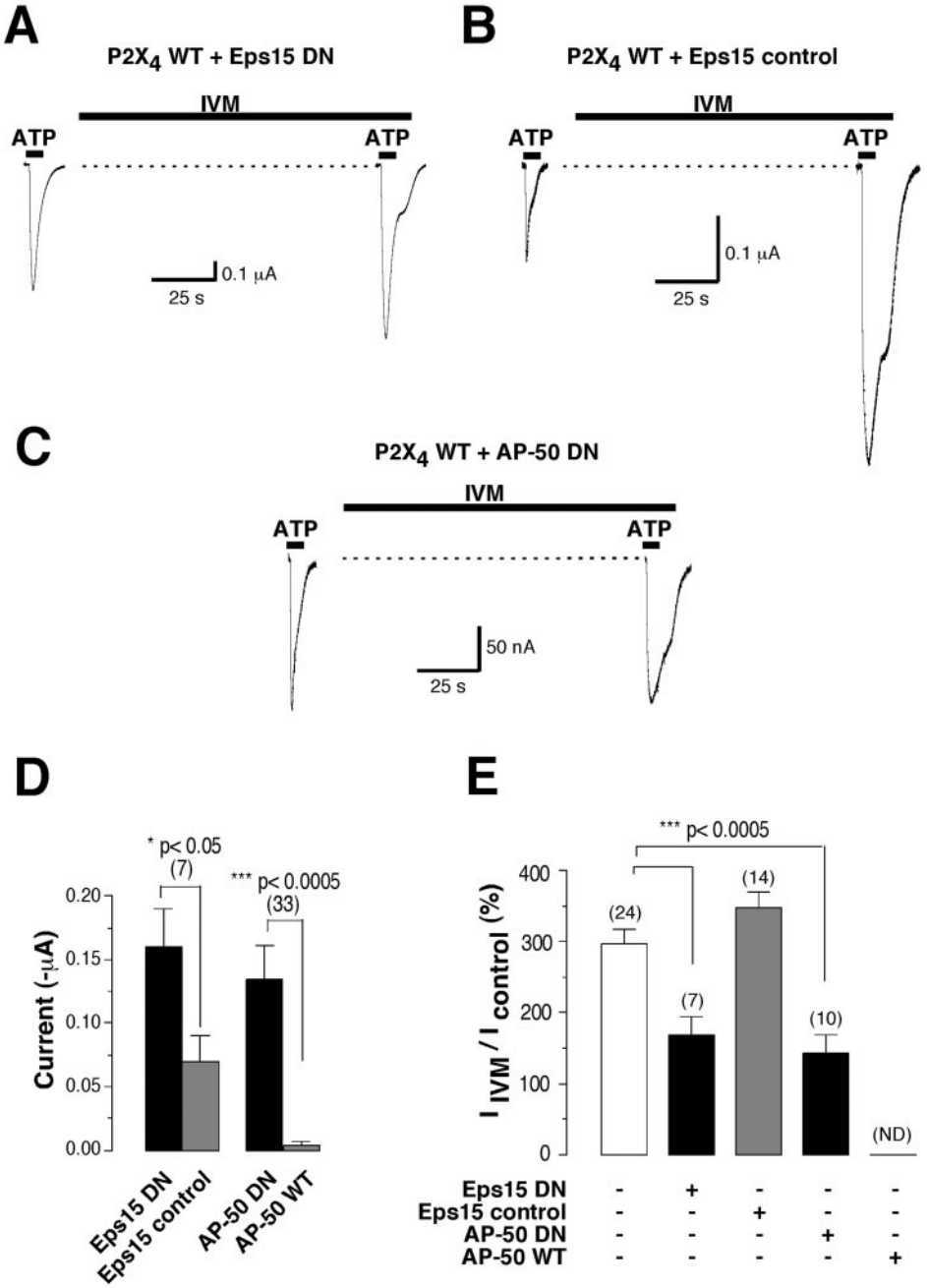

Fig. 6. Potentiation of P2X$_4$ WT peak current is dependent on clathrin-dependent endocytosis. A, B, and C, representative 100 μM ATP currents before and after ivermectin preincubation from oocytes coexpressing P2X$_4$ WT receptors with either the dominant-negative mutant of Eps15 (A), a control form of Eps15 (B), or the dominant-negative mutant of AP-50 (C). D, means of amplitude of initial ATP responses showed that expression of P2X$_4$ WT receptors was significantly higher in the presence of Eps15 DN or AP-50 DN than in the presence of their respective protein control (*, $p < 0.05$; ***, $p < 0.0005$). E, histograms showing the effect of ivermectin on normalized ATP-induced currents in oocytes expressing P2X$_4$ WT channels plus control or DN Eps15 as well as wild-type or DN AP-50. The expression of both dominant-negative of clathrin-mediated endocytosis significantly decreased the potentiation of P2X$_4$ WT currents by IVM (***, $p < 0.0005$). ND, not determined.

curve (Krause et al., 1998). This prompted us to investigate ivermectin action mechanism on nα7ACh receptors. We expressed rat nα7AChR in *X. laevis* oocytes and showed that 20-s preapplication of ivermectin (30 μM) induced a large and reversible increase (219 ± 13%, n = 13; Fig. 7, A and B) of current evoked by application of ACh (300 μM). To explore further the mechanism of potentiation, we examined the functional consequences of the disruption of clathrin-dependent pathway using the dominant-negative mutants mentioned above. In oocytes coexpressing nα7ACh receptors and the dominant-negative Eps15 mutant, ivermectin potentiation was significantly reduced (152.7 ± 9%, n = 18). On the

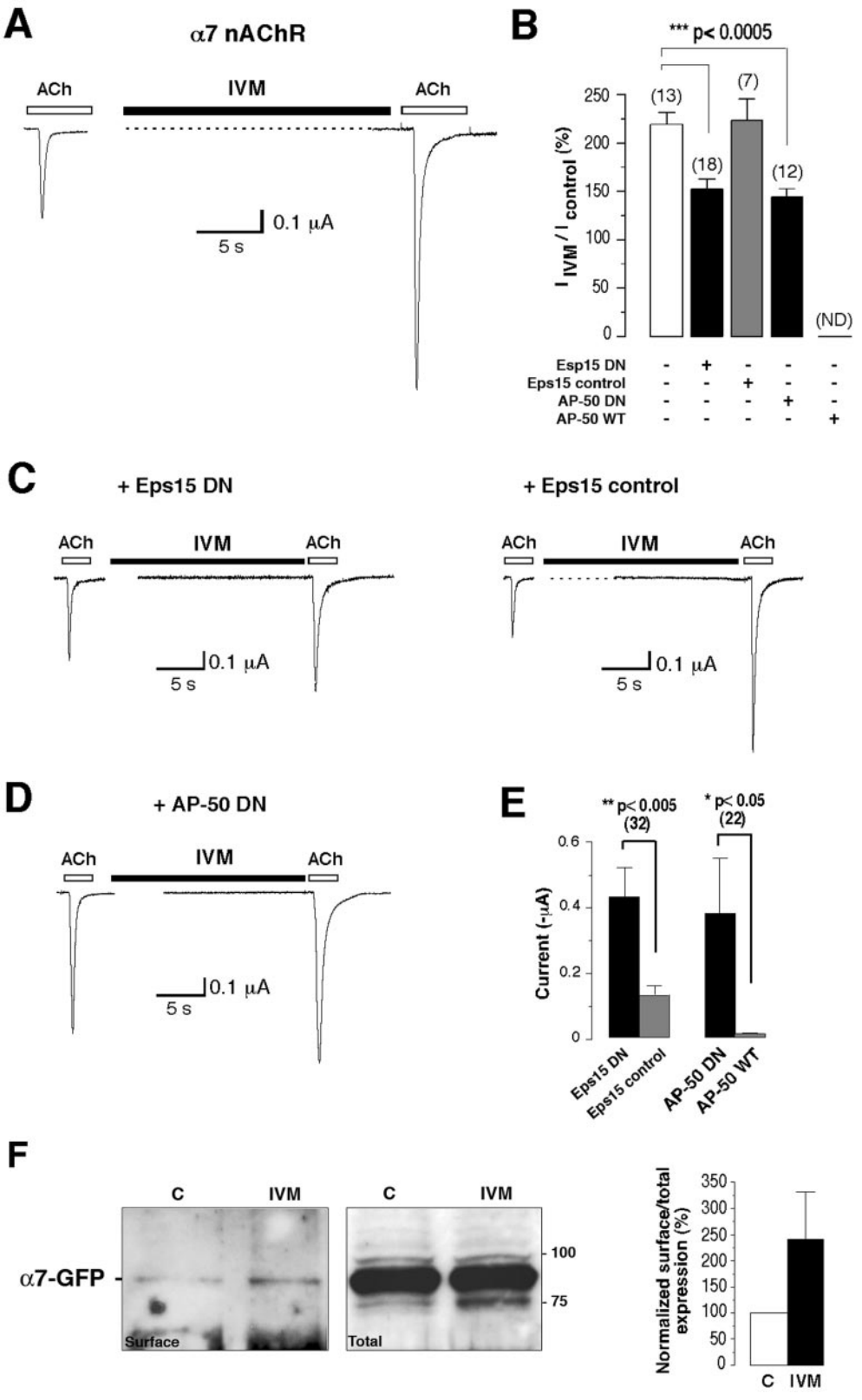

Fig. 7. Ivermectin increases surface expression of nα7ACh receptors by a mechanism dependent on clathrin-dependent endocytosis. A, C, and D, ACh-evoked currents (300 μM) before and after 20-s application of 30 μM ivermectin (IVM) from oocytes expressing nα7ACh receptors alone (A) and in combination either with control or DN Eps15 (C) or wild-type or DN AP-50 (D). B, histogram illustrating that the 2-fold potentiation of nα7ACh currents by ivermectin is significantly decreased in the presence of the dominant-negative mutants of Eps15 or AP-50 proteins. E, means of the amplitude of ACh responses showing that expression of nα7ACh receptors is higher in the presence of the dominant-negative mutants compared with the respective control proteins. F, surface expression of nα7ACh-GFP receptors is increased by ivermectin. GFP-tagged nα7ACh receptors expressing oocytes were incubated in IVM (30 μM) or in DMSO (c) 2 min before surface biotinylation. Immunoblot probes with anti-GFP antibodies shows that treatment by ivermectin increases the surface biotinylated fraction, whereas total fraction remains unchanged.

contrary, ivermectin was still able to potentiate nα7AChR current evoked by ACh in the presence of Eps15 control (223.9 ± 22.6%; Fig. 7, B and C). The amplitude of ACh currents was significantly different in the presence of either Eps15 DN or Eps15 control, demonstrating the expression of the dominant-negative mutant (Fig. 7, C and E).

Likewise, coexpression of nα7AChR and AP-50 DN also significantly reduced up-regulation of ACh currents by ivermectin. After preincubation with ivermectin, ACh currents represented 144.4 ± 8.35% (n = 12) of control currents (Fig. 7, B and D). Similar to $P2X_4$ receptors in oocytes coexpressing wild-type AP-50 and nα7ACh receptors, ACh currents were rarely measurable, whereas in the presence of the dominant-negative AP-50 DN mutant, the amplitude of ACh currents was significantly higher (Fig. 7E). Thus, the functional up-regulation of nα7ACh receptors by ivermectin did not occur when endocytosis was prevented.

To examine the surface expression of nα7ACh receptors, we expressed GFP-tagged α7 receptors (α7-GFP) in oocytes. We first verified that ivermectin potentiated α7-GFP receptor ACh current (not shown). Biotinylation and anti-GFP Western blot experiments showed that 2-min preincubation of oocytes expressing α7-GFP with 30 μM ivermectin increased the surface signal (by 240 ± 90%, two independent experiments; Fig. 7F). The surface fraction of α7-GFP subunits was estimated at ~0.3% of total α7-GFP subunits in control conditions (incubation in 0.3% DMSO), revealing a weak surface expression. Overall, these experiments demonstrated that functional up-regulation of nα7AChR by ivermectin can be accounted for by an increase in the number of surface receptors, which involves nα7ACh receptor endocytosis.

Discussion

Like many ligand-gated channels, including $GABA_A$ and AMPA receptors (Carroll et al., 2001), $P2X_4$ receptors, but not other P2X subtypes tested so far, undergo rapid constitutive internalization by clathrin-dependent endocytosis and subsequent reinsertion into the plasma membrane (Bobanovic et al., 2002). The recruitment of $P2X_4$ channels to clathrin-coated pits is ensured by the direct association between a nontraditional tyrosine-based sorting signal in the cytosolic C-terminal tail of $P2X_4$ subunits and AP-50 (also called μ2) subunits of AP2 complexes (Royle et al., 2002, 2005). In this study, we show that disruption of the internalization signal of rat and human $P2X_4$ subunits induced a large increase in the amplitude of ATP-elicited current compared with $P2X_4$ WT currents by facilitating surface expression. According to previous studies on P2X trafficking in transfected neurons or HEK cells (Bobanovic et al., 2002), the disruption of the internalization motif results in an increase in the number of cell surface channels, indicating that a similar mechanism governs internalization of $P2X_4$ receptors in *X. laevis* oocytes.

Loss of Association with AP2 Produces Unique $P2X_4$ Functional Properties. Recombinant mammalian $P2X_4$ receptors are moderately desensitizing ATP-gated channels, insensitive to $\alpha\beta$-methylene-ATP (Garcia-Guzman et al., 1997; Jones et al., 2000; North, 2002), and specifically potentiated by ivermectin (Khakh et al., 1999b; Priel and Silberberg, 2004). Internalization-deficient $P2X_4$ channels displayed a 15-fold increase in the apparent sensitivity to ATP (Fig. 2), a higher ionic permeability (Fig. 3), and in addition, these mutant receptors were not potentiated by ivermectin (Fig. 4). Previous studies demonstrated that high expression levels in transfected cells modify kinetics or agonist sensitivity of other ligand-gated channels such as $P2X_2$ or glycine receptors (Legendre et al., 2002; Fujiwara and Kubo, 2004). In this study, we took the precaution to reduce the expression of mutants to the level of wild-type $P2X_4$ receptors. Therefore, the modulation of $P2X_4$ channel properties, not attributable to channel density-dependent changes, is likely to be a direct consequence of the loss of interaction between AP2 complexes and the C terminus of $P2X_4$ receptors. Loss of interaction between microtubule-associated protein 1B and $GABA_C$ receptors was also shown to increase the GABA sensitivity of $GABA_C$ receptors (Billups et al., 2000). In our study, a higher responsiveness to $\alpha\beta$-methylene-ATP was also observed but only at high channel density. Thus, contrary to other changes, the increase of $\alpha\beta$-methylene-ATP potency may result from self-interaction or positive cooperation promoted by the aggregation of $P2X_4$ channels.

$P2X_4$ receptors change their ion selectivity: they open a small pore (I_1 state) in milliseconds and during prolonged exposure to agonists operate a transition toward a larger pore (I_2 state; Khakh et al., 1999a). In a low-Ca^{2+} solution, internalization-deficient $P2X_4$ channels displayed biphasic kinetics during prolonged ATP application, although I_2/I_1 ratio was significantly reduced. Determination of $NMDG^+/Na^+$ permeability changes revealed that I_1 state of $P2X_4$ Y378A channels was highly permeable to $NMDG^+$ compared with wild-type $P2X_4$ channels. Fisher et al. (2004) demonstrated that the cytosolic domain of $P2X_2$ undergoes a conformational rearrangement correlating with permeability changes. It would be of interest to determine whether or not the loss of interaction between AP2 complex and $P2X_4$ channels promotes C terminus motion, leading to the opening in milliseconds of a highly permeable pore. It remains unclear why $P2X_4$ Y378A channels developed a (smaller) second current phase when no significant increase or decrease in $NMDG^+$ permeability was noticed. Further investigations using $P2X_4$ Y378A receptors could be helpful to decipher mechanistic and dynamic aspects of the transition between both states.

Properties of Internalization-Deficient $P2X_4$ Channels Are Consistent with Those of Central ATP Responses. It is noteworthy that $P2X_4$ is the most widely distributed P2X subunit in the central nervous system (Norenberg and Illes, 2000; Bo et al., 2003). However, native P2X receptor phenotypes in the brain do not resemble heterologously expressed homo/heteromeric $P2X_4$ channels (North, 2002). For instance, in brainstem, habenula, or CA1 neurons, ATP- and $\alpha\beta$-methylene-ATP-evoked currents are partially inhibited by suramin (Khakh et al., 1999b; Pankratov et al., 2002). Ivermectin does not modulate ATP-evoked current in brainstem or CA1 neurons (Khakh et al., 1999b), brain regions in which $P2X_4$ transcripts and/or proteins are abundant (Norenberg and Illes, 2000; Rubio and Soto, 2001). Kinetic and pharmacological properties of internalization-deficient $P2X_4$ channels described in this work are consistent with the phenotype of native P2X responses in many areas of the brain, suggesting that homomeric $P2X_4$ receptors may play an important role in fast ATP synaptic transmission.

This implies that cellular processes (Traub, 2003) probably control interactions between the endocytic machinery and $P2X_4$ receptors and, consequently, the surface expression and function of synaptic $P2X_4$ receptors.

Mode of $P2X_4$ or nα7ACh Receptors Potentiation by Ivermectin. Ivermectin increases ATP-evoked currents through rat and human $P2X_4$ channels and slows their deactivation in transfected HEK cells, oocytes, or neurons, but not through other P2X subtypes. In addition, in the presence of ivermectin, the ATP concentration-response curve is shifted to the left, and $\alpha\beta$-methylene-ATP becomes a potent agonist of $P2X_4$ channels (Khakh et al., 1999b; Priel and Silberberg, 2004). Ivermectin has been described as a positive allosteric modulator with two potential binding sites on $P2X_4$ channels: a high-affinity site increases the maximum current, and a lower affinity site slows deactivation and increases apparent affinity for ATP (Priel and Silberberg, 2004). However, neither the binding sites nor the allosteric mechanism have been elucidated. In this study, we observed a 3-fold potentiation of maximum ATP current for rat and human $P2X_4$ WT channels, whereas $P2X_4$ Y378A or $P2X_4$ Δ377 channels of both species were not potentiated by ivermectin. However, ivermectin slows deactivation of both wild-type and mutated channels. Our data are consistent with the fact that changes in deactivation kinetics and up-regulation by ivermectin arise from two distinct mechanisms (Priel and Silberberg, 2004) and suggested a link between action of ivermectin and receptor internalization.

Biotinylation/immunoblotting experiments demonstrate that ivermectin treatment causes a 3- to 4-fold increase in the number of plasma membrane $P2X_4$ WT receptors without changing the total number of receptors. On the other hand, ivermectin does not change the surface expression of internalization-deficient receptors. Moreover, disruption of clathrin-dependent endocytosis by the expression of dominant-negative mutant of Eps15 or AP-50 protein prevented the potentiation of ATP current of $P2X_4$ WT receptors. Overall, these results demonstrated that the potentiation by ivermectin of $P2X_4$ current amplitude is attributable to receptors newly inserted into the plasma membrane by an endocytosis-dependent mechanism. Given that 1) ivermectin acts rapidly (2-min treatment), reversibly without changing the membrane capacitance (Khakh et al., 1999b), and 2) $P2X_4$ channels rapidly cycle in and out of the membrane (Bobanovic et al., 2002), it is tempting to speculate that ivermectin impairs $P2X_4$ receptor recruitment to coated pits via AP2 proteins (without preventing the formation of endocytic vesicles), which lead to the reinsertion into the plasma membrane of $P2X_4$ receptors from intracellular pools. Such an interpretation implies that during ivermectin treatment, surface $P2X_4$ receptors do not interact with AP2 complexes. This is in agreement with the finding that loss of interaction with AP2 complex conferred to $P2X_4$ receptors properties, which resemble those described in the presence of ivermectin (Khakh et al., 1999b). However, further studies will be necessary to bring direct evidence that the extracellular binding of ivermectin onto $P2X_4$ channels disrupts interaction with AP2 proteins. Although previous studies showed the constitutive endocytosis of $P2X_4$-GFP in HEK cells (Bobanovic et al., 2002), we noted that C-terminal-tagged $P2X_4$ receptors expressed in oocytes were less potentiated by ivermectin than wild-type $P2X_4$ receptors. A plausible explanation for these discrepancies is that fluorescent protein linked to the end of the short C terminus of $P2X_4$ subunits disturbs AP2/clathrin endocytosis in oocytes.

It remains to be determined whether an endogenous effector binds to ivermectin sites to regulate interaction between AP2 and $P2X_4$ channels. Such regulation may explain the ivermectin insensitivity of native $P2X_4$ channels (Khakh et al., 1999b) and the fact that ivermectin, widely used in human medicine against tropical filarial diseases, is well tolerated (Twum-Danso, 2003).

Ivermectin modulates other ligand-gated channels including $GABA_A$ and nα7ACh receptors (Krusek and Zemkova, 1994; Krause et al., 1998). Here we demonstrated that, similarly to $P2X_4$ receptors, ivermectin increases the number of surface nα7ACh receptors by a mechanism dependent on clathrin/AP2-mediated endocytosis in *X. laevis* oocytes. These findings suggest that binding of ivermectin on the extracellular domain of distinct receptor-channels (such as $GABA_A$ receptors, nα7AChR) leads to the impairment of their constitutive internalization. Indeed, $GABA_A$ receptors are recruited in clathrin-coated pits by interaction between dileucine or atypical signals and AP2 proteins (Herring et al., 2003). Despite recent findings showing a tyrosine kinase-dependent regulation of the surface receptor density, regulation of surface nα7ACh receptors and their internalization signals remains to be identified (Cho et al., 2005). Our results, showing the increase in nα7ACh receptor expression in the presence of the dominant-negative mutant of Eps15 or AP-50, constitute the first indication that nα7ACh receptors undergo constitutive internalization by a clathrin-dependent pathway.

Acknowledgments

We thank Dr. Philippe Séguéla for providing rat nα7AChR clones and Dr. Agnès Hémar for the dominant-negative mutants of Eps15cDNAs.

References

Benmerah A, Begue B, Dautry-Varsat A, and Cerf-Bensussan N (1996) The ear of α-adaptin interacts with the COOH-terminal domain of the Eps 15 protein. *J Biol Chem* **271:**12111–12116.

Billups D, Hanley JG, Orme M, Attwell D, and Moss SJ (2000) GABAC receptor sensitivity is modulated by interaction with MAP1B. *J Neurosci* **20:**8643–8650.

Bobanovic LK, Royle SJ, and Murrell-Lagnado RD (2002) P2X receptor trafficking in neurons is subunit specific. *J Neurosci* **22:**4814–4824.

Boué-Grabot E, Archambault V, and Seguela P (2000) A protein kinase C site highly conserved in P2X subunits controls the desensitization kinetics of $P2X_2$ ATP-gated channels. *J Biol Chem* **275:**10190–10195.

Boué-Grabot E, Emerit MB, Toulme E, Seguela P, and Garret M (2004a) Cross-talk and co-trafficking between rho1/GABA receptors and ATP-gated channels. *J Biol Chem* **279:**6967–6975.

Boué-Grabot E, Toulme E, Emerit MB, and Garret M (2004b) Subunit-specific coupling between γ-aminobutyric acid type A and P2X2 receptor channels. *J Biol Chem* **279:**52517–52525.

Bowie D, Garcia EP, Marshall J, Traynelis SF, and Lange GD (2003) Allosteric regulation and spatial distribution of kainate receptors bound to ancillary proteins. *J Physiol* **547:**373–385.

Bo X, Kim M, Nori SL, Schoepfer R, Burnstock G, and North RA (2003) Tissue distribution of P2X4 receptors studied with an ectodomain antibody. *Cell Tissue Res* **313:**159–165.

Carroll RC, Beattie EC, von Zastrow M, and Malenka RC (2001) Role of AMPA receptor endocytosis in synaptic plasticity. *Nat Rev Neurosci* **2:**315–324.

Chen L, Wang H, Vicini S, and Olsen RW (2000) The gamma-aminobutyric acid type A (GABAA) receptor-associated protein (GABARAP) promotes GABAA receptor clustering and modulates the channel kinetics. *Proc Natl Acad Sci USA* **97:**11557–11562.

Cho CH, Song W, Leitzell K, Teo E, Meleth AD, Quick MW, and Lester RA (2005) Rapid upregulation of alpha7 nicotinic acetylcholine receptors by tyrosine dephosphorylation. *J Neurosci* **25:**3712–3723.

Cully DF, Vassilatis DK, Liu KK, Paress PS, Van der Ploeg LH, Schaeffer JM, and Arena JP (1994) Cloning of an avermectin-sensitive glutamate-gated chloride channel from Caenorhabditis elegans. *Nature (Lond)* **371:**707–711.

Ennion SJ and Evans RJ (2002) Conserved cysteine residues in the extracellular loop

of the human P2X$_1$ receptor form disulfide bonds and are involved in receptor trafficking to the cell surface. *Mol Pharmacol* **61:**303–311.
Fisher JA, Girdler G, and Khakh BS (2004) Time-resolved measurement of state-specific P2X2 ion channel cytosolic gating motions. *J Neurosci* **24:**10475–10487.
Fujiwara Y and Kubo Y (2004) Density-dependent changes of the pore properties of the P2X2 receptor channel. *J Physiol* **558:**31–43.
Garcia-Guzman M, Soto F, Gomez-Hernandez JM, Lund PE, and Stuhmer W (1997) Characterization of recombinant human P2X4 receptor reveals pharmacological differences to the rat homologue. *Mol Pharmacol* **51:**109–118.
Herring D, Huang R, Singh M, Robinson LC, Dillon GH, and Leidenheimer NJ (2003) Constitutive GABAA receptor endocytosis is dynamin-mediated and dependent on a dileucine AP2 adaptin-binding motif within the β2 subunit of the receptor. *J Biol Chem* **278:**24046–24052.
Jones CA, Chessell IP, Simon J, Barnard EA, Miller KJ, Michel AD, and Humphrey PP (2000) Functional characterization of the P2X(4) receptor orthologues. *Br J Pharmacol* **129:**388–394.
Khakh BS, Bao XR, Labarca C, and Lester HA (1999a) Neuronal P2X transmitter-gated cation channels change their ion selectivity in seconds. *Nat Neurosci* **2:**322–330.
Khakh BS, Proctor WR, Dunwiddie TV, Labarca C, and Lester HA (1999b) Allosteric control of gating and kinetics at P2X(4) receptor channels. *J Neurosci* **19:**7289–7299.
Kittler JT, Delmas P, Jovanovic JN, Brown DA, Smart TG, and Moss SJ (2000) Constitutive endocytosis of GABAA receptors by an association with the adaptin AP2 complex modulates inhibitory synaptic currents in hippocampal neurons. *J Neurosci* **20:**7972–7977.
Krause RM, Buisson B, Bertrand S, Corringer PJ, Galzi JL, Changeux JP, and Bertrand D (1998) Ivermectin: a positive allosteric effector of the α7 neuronal nicotinic acetylcholine receptor. *Mol Pharmacol* **53:**283–294.
Krusek J and Zemkova H (1994) Effect of ivermectin on gamma-aminobutyric acid-induced chloride currents in mouse hippocampal embryonic neurones. *Eur J Pharmacol* **259:**121–128.
Legendre P, Muller E, Badiu CI, Meier J, Vannier C, and Triller A (2002) Desensitization of homomeric α1 glycine receptor increases with receptor density. *Mol Pharmacol* **62:**817–827.
Le KT, Villeneuve P, Ramjaun AR, McPherson PS, Beaudet A, and Seguela P (1998) Sensory presynaptic and widespread somatodendritic immunolocalization of central ionotropic P2X ATP receptors. *Neuroscience* **83:**177–190.
Mayer ML (2005) Glutamate receptor ion channels. *Curr Opin Neurobiol* **15:**282–288.
Moss SJ and Smart TG (2001) Constructing inhibitory synapses. *Nat Rev Neurosci* **2:**240–250.
Nesterov A, Carter RE, Sorkina T, Gill GN, and Sorkin A (1999) Inhibition of the receptor-binding function of clathrin adaptor protein AP-2 by dominant-negative mutant mu2 subunit and its effects on endocytosis. *EMBO (Eur Mol Biol Organ) J* **18:**2489–2499.
Nicke A, Kerschensteiner D, and Soto F (2005) Biochemical and functional evidence for heteromeric assembly of P2X1 and P2X4 subunits. *J Neurochem* **92:**925–933.
Norenberg W and Illes P (2000) Neuronal P2X receptors: localisation and functional properties. *Naunyn-Schmiedeberg's Arch Pharmacol* **362:**324–339.
North RA (2002) Molecular physiology of P2X receptors. *Physiol Rev* **82:**1013–1067.
Pankratov YV, Lalo UV, and Krishtal OA (2002) Role for P2X receptors in long-term potentiation. *J Neurosci* **22:**8363–8369.
Priel A and Silberberg SD (2004) Mechanism of ivermectin facilitation of human P2X4 receptor channels. *J Gen Physiol* **123:**281–293.
Royle SJ, Bobanovic LK, and Murrell-Lagnado RD (2002) Identification of a non-canonical tyrosine-based endocytic motif in an ionotropic receptor. *J Biol Chem* **277:**35378–35385.
Royle SJ, Qureshi OS, Bobanovic LK, Evans PR, Owen DJ, and Murrell-Lagnado RD (2005) Non-canonical YXXGϕ endocytic motifs: recognition by AP2 and preferential utilization in P2X4 receptors. *J Cell Sci* **118:**3073–3080.
Rubio ME and Soto F (2001) Distinct localization of P2X receptors at excitatory postsynaptic specializations. *J Neurosci* **21:**641–653.
Soto F, Garcia-Guzman M, Gomez-Hernandez JM, Hollmann M, Karschin C, and Stuhmer W (1996) P2X4: an ATP-activated ionotropic receptor cloned from rat brain. *Proc Natl Acad Sci USA* **93:**3684–3688.
Traub LM (2003) Sorting it out: AP-2 and alternate clathrin adaptors in endocytic cargo selection. *J Cell Biol* **163:**203–208.
Twum-Danso NA (2003) Serious adverse events following treatment with ivermectin for onchocerciasis control: a review of reported cases. *Filaria J* **2 (Suppl 1):**S3.
Virginio C, MacKenzie A, Rassendren FA, North RA, and Surprenant A (1999) Pore dilation of neuronal P2X receptor channels. *Nat Neurosci* **2:**315–321.

Address correspondence to: Dr. Eric Boué-Grabot, Centre National de la Recherche Scientifique Unité Mixte de Recherche 5543, Université Victor Segalen Bordeaux2, 146 rue Léo Saignat, 33076 Bordeaux cedex, France. E-mail: eric.boue-grabot@umr5543.u-bordeaux2.fr